

Cache-aware Performance Modeling and Prediction for Dense Linear Algebra

Elmar Peise and Paolo Bientinesi

Aachen Institute
for Advanced Study in
Computational Engineering Science

Financial support from the
Deutsche Forschungsgemeinschaft (German Research Foundation)
through grant GSC 111 is gratefully acknowledged.

Cache-aware Performance Modeling and Prediction for Dense Linear Algebra

Elmar Peise and Paolo Bientinesi

AICES, RWTH Aachen
{peise,pauldj}@aices.rwth-aachen.de

Abstract. Countless applications cast their computational core in terms of dense linear algebra operations. These operations can usually be implemented by combining the routines offered by standard linear algebra libraries such as BLAS and LAPACK, and typically each operation can be obtained in many alternative ways. Interestingly, identifying the fastest implementation—without executing it—is a challenging task even for experts. An equally challenging task is that of tuning each routine to performance-optimal configurations. Indeed, the problem is so difficult that even the default values provided by the libraries are often considerably suboptimal; as a solution, normally one has to resort to executing and timing the routines, driven by some form of parameter search. In this paper, we discuss a methodology to solve both problems: identifying the best performing algorithm within a family of alternatives, and tuning algorithmic parameters for maximum performance; in both cases, we do not execute the algorithms themselves. Instead, our methodology relies on timing and modeling the computational kernels underlying the algorithms, and on a technique for tracking the contents of the CPU cache. In general, our performance predictions allow us to tune dense linear algebra algorithms within few percents from the best attainable results, thus allowing computational scientists and code developers alike to efficiently optimize their linear algebra routines and codes.

1 Introduction

Most dense linear algebra (DLA) operations can be computed via multiple alternative algorithms (“variants”), the performance of which can normally be tuned by one or more configuration parameters. Since the performance of these algorithms depends on a variety of factors, including the problem size, the target architecture, and the underlying libraries, selecting the optimal combination of variant and configuration parameters becomes a real challenge. However, such algorithms, including many covered by the Linear Algebra PACKage (LAPACK) [1], achieve their efficiency by building on a rather small set of highly tuned kernels, most of which are provided by the Basic Linear Algebra Subprograms (BLAS) [2–4]. Given a linear algebra algorithm \mathcal{A} consisting of such kernels, we aim at predicting \mathcal{A} ’s performance, *without ever executing it*. Our approach relies on the typical layered structure of DLA libraries and on their

data-independent program flow;¹ as a constraint, we only allow the execution of the kernels, and not of the algorithm itself.

In a nutshell, our approach consists of two stages: 1) generation of accurate performance models for the computational building blocks (kernels) and, to effectively use those models, 2) tracking the state of the CPU’s cache throughout the target algorithm. In this paper, we extend and integrate our work on automated performance modeling [5], which only considered in-cache operations, with that on cache tracking [6], in order to construct reliable performance predictions for a spectrum of problem sizes, ranging from small problems fitting in cache, to large ones that can only reside in main memory. We show that highly accurate time predictions for dense linear algebra algorithms are attainable, and that such estimates are so close to the observed performance, that it becomes possible not only to correctly rank the algorithms, but to also tune their implementation without executing them.

We motivate here our work by means of a typical scenario. In order to exploit BLAS-3 performance, many of LAPACK’s routines employ blocked algorithms; these algorithms work not with scalar and vector matrix portions, but always with blocks and panels of a predefined *block-size* b —a crucial optimization parameter. In Fig. 1, we illustrate the impact of this block-size on the performance of LAPACK’s QR and Cholesky decompositions (respectively, `dgeqrf` and `dpotrfL`): We use one core of an Intel Penryn E5450² (Harpertown) and link LAPACK to the high-performance OPENBLAS library [7] to decompose square matrices of size $n = 3,800$ with varying block-size b . As the figure shows, optimal performance for `dgeqrf` (QR) is attained with $b = 112$; by contrast, LAPACK’s default value is $b = 32$, for which `dgeqrf` is 15% slower. For `dpotrfL` (Cholesky), the message is similar: when using LAPACK’s default $b = 64$, the decomposition takes 13% longer than for the optimal value at $b = 384$. One of the applications of the methodology presented in this paper is to automatically tuning algorithmic parameters such as these block-sizes without the here presented empirical experiments.

There exist several works on performance modeling and on the influence of caching in DLA; we mention here some notable examples. Cuenca et al. developed a system of self-optimizing linear algebra routines (SOLAR) [8]; every routine is associated with performance information, which is hierarchically propagated to higher level routines in order to tune them. Iakymchuk et al. model the performance of BLAS analytically based on memory access patterns [9, 10]; while their models represent the program execution very accurately, constructing them requires a high level of expertise of both routines and architecture. Whaley empirically tunes the block-size for LAPACK routines and emphasizes its impact on performance [11]. Lam et al. study caching in the context of blocking within DLA kernels [12].

¹ Eigensolvers are an exception, since their program flow always depends on the input data.

² 3GHz, 4 cores, 6MB L2 cache per 2 cores, 4 flops/cycle.

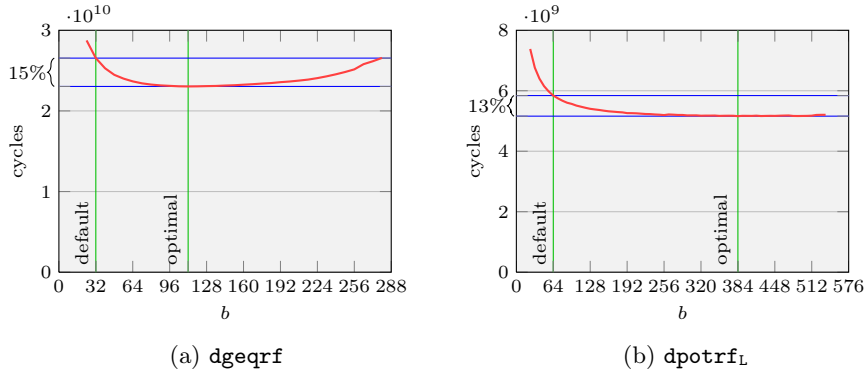


Fig. 1: Runtime of `dgeqrf` (QR) and `dpotrfL` (Cholesky) on square matrices of size $n = 3,800$ with varying block-size b .

In contrast, our approach combines highly accurate, measurement based performance models for compute kernel with an automated analysis of the cache states present throughout the algorithm execution. With this combination, we extend our work on model-based performance predictions [5] from in-cache problem sizes to the significantly more challenging scenario of problems not fitting in cache.

The rest of this paper is structured as follows: In [Sec. 2](#), we detail our performance modeling technique for DLA kernels. In [Sec. 3](#), we introduce our cache prediction model and its application in conjunction with performance models to predict DLA algorithms. In [Sec. 4](#), we present prediction results and use such predictions to tune several operations.

2 Performance Modeling

In this section we give an overview of our automated performance modeling framework for dense linear algebra kernels. Given an architecture and implementations of the kernel routines (e.g., a BLAS library), this framework, first introduced in [5], automatically performs a series of performance measurements to construct a performance model for each kernel. Given a set of routine arguments, such a model then yields accurate execution time estimates.

2.1 Treatment of Kernel Arguments and Model Structure

The first step towards constructing performance models of high quality is to identify the routine features that the models shall capture. For this purpose, let us consider the exemplary BLAS kernel `dtrsm`—the double precision solve of a triangular linear system with multiple right hand sides ($B := A^{-1}B$). This kernel’s interface is not only prototypical for other kernels, it contains all relevant types of arguments:

`dtrsm(side, uplo, transA, diag, m, n, alpha, A, ldA, B, ldB)`

Before studying how these arguments affect the kernel performance, we give a quick overview of their semantics.

- `side`, `uplo`, `transA`, and `diag` are *flag arguments*. They identify the precise form of the linear system that is solved: The side on which A appears, whether A is lower or upper triangular, whether A is transposed, and whether A is unit-triangular.
- `m` and `n` are *size arguments*: $B \in \mathbb{R}^{m \times n}$ and A correspondingly.
- `alpha` is a *scalar argument* that scales the whole linear system: $B := \alpha A^{-1} B$.
- `A` and `B` are *data arguments* or *operands*; they point to the first entries of, respectively, A and B .
- `ldA` and `ldB` are *leading dimension arguments* corresponding to A and B . While the columns of these matrices are stored contiguously (stride 1), the distances of elements of a matrix row are given by the leading dimensions (strides `ldA` and `ldB`). Distinguishing these row strides from the matrix heights allows to operate on sub-matrices, i.e., parts of larger matrices.

We now decide how to represent these arguments in our models by considering their individual impact on the kernel performance.

- **Flag arguments** are limited to few discrete values. Depending on these values, however, the kernel implementation may trigger entirely different execution branches with completely independent performance characteristics. To account for these individual characteristics, we create a separate performance model for each relevant combination of flag arguments (except `diag`).³
- **Size arguments** determine the amount of computation and thus clearly affect performance. To account for fine implementation and hardware dependent performance characteristics, we used not a single but piecewise polynomials to these arguments' impact on execution time.
- **Scalar arguments** at first sight do not change the computation significantly. However, some special values—namely -1 , 0 , and 1 —may, trigger separate execution branches in the same way that flag arguments do to avoid redundant multiplications. Hence, we also treat these values just like flag arguments, creating a separate model for each special value and one for the general case.
- **Data arguments**: With few exceptions (such as eigensolvers), the executed instructions and thus the performance of dense linear algebra kernels do not depend on their operands. However, performance may depend significantly on such arguments' cache locality; kernels will execute faster when their operands are in cache. We reduce the generally arbitrarily large set of cache preconditions to two extreme cases, where either all operands are *in-cache* or they all only reside in main memory (*out-of-cache*). Ensuring these cache locality conditions while taking measurements, we create two separate models for these two cases.

³ in practice, only a limited set of flag combinations is encountered.

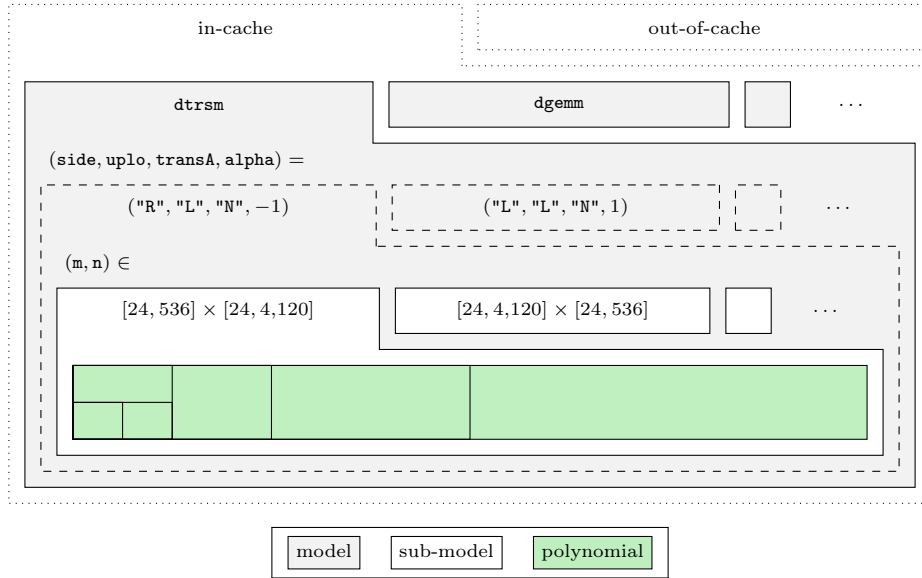


Fig. 2: Structure of the performance models.

- **Leading dimension arguments** change the memory access strides when kernels load multiple columns of a matrix simultaneously. While these strides may affect kernel performance slightly for small operands, we do not cover their influence in our models and assume large leading dimensions, reflecting the common use-case of kernels invocations on sub-matrices.

The structure of our performance models is summarized in Fig. 2: For each routine we will have two entirely separate models for in- and out-of-cache situations. Each of these models is in turn constructed of a set of *sub-models*—one for each combination of flag and special scalar argument values. Each sub-model is now only concerned with modeling execution time as a function of the kernel’s size arguments. Structurally, these models are multivariate piecewise polynomials dividing the space spanned by the size arguments (which is in practice up to 3-dimensional).

2.2 Adaptive Refinement

Let us consider how sub-models are generated for the space spanned by the size argument(s): starting with a designated rectangular⁴ subspace, (or possibly several distinct sub-spaces), a subdivision is dynamically obtained through adaptive refinement. The approach begins by taking execution time samples on a regular grid spanning the entire considered subspace; in order to establish a stable basis

⁴ In the 2-dimensional case; generally: hyper-cuboidal.

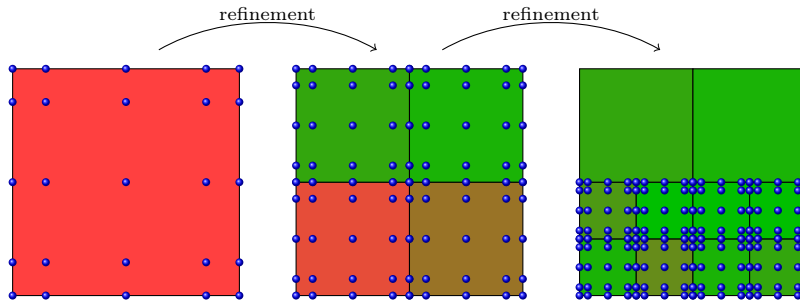


Fig. 3: Adaptive refinement and sample point selection (\bullet).

for the model, this sampling is repeated multiple times per grid point and the median time is used. Least squares fitting is then used to generate a multivariate polynomial which constitutes a first approximation to the execution time. In most cases, this approximation is far too coarse to be acceptable; specifically, if the error between the least squares fitted polynomial and the samples on the grid is above a certain threshold, the subspace is subdivided into roughly equally sized quadrants. The process of sampling, least squares fitting, and conditionally subdividing the space is repeated iteratively until a termination criterion (accuracy or refinement depth) is met.

Example 1. An illustration of this adaptive refinement process is given in Fig. 3 from left to right. In the beginning, a coarse grid of sampling points (\bullet) yields a first polynomial approximation of the routine’s performance. However, since this approximation does not satisfy the accuracy requirements (indicated by the color), the space is subdivided into equally sized quadrants (Fig. 3, middle). In each quadrant a new set of sampling points is chosen and new a new polynomial approximation is least squares fitted. In this example, this approximation is already sufficiently accurate for the upper quadrants, while the lower quadrants are further subdivided and the refinement is recursively repeated. Subsequent refinement steps could further subdivide these resulting quadrants until the refinement’s termination criteria are reached.

Our performance modeling framework has several configuration parameters, which guide the adaptive refinement based model generation and influence the trade-off between model accuracy and the number of required samples (and thus the time spent on generating the models). In the following we list these parameters along with the empirical values⁵ we use for them in the remainder of this paper:

⁵ These values assure an excellent model accuracy for a reasonable number of samples across various scenarios, such as involving different hardware and libraries.

- To avoid small-scale performance fluctuations in the size arguments, the coordinates of all sampling points are rounded to multiples of a *minimum width* of 8.
- When sampling a sub-space, we choose the *sampling grid* as the Cartesian products of Gaussian points along each of its dimensions (\bullet in Fig. 3). Compared to alternatives such as a regularly spaced grid or a grid refined on its boundaries, this choice has shown to yield the highest accuracy.
- The *target error bound* for our models (the first refinement termination criterion) is chosen at 5%. Since this is an upper bound, in practice the resulting models will have a significantly higher accuracy.
- The *minimum size* of sub-spaces (the second termination criterion) is limited to 32 along each of the space’s dimensions.
- Our least squares fitter uses polynomials of *polynomial degree* 3.
- To fit polynomials of degree n , one needs at least $n + 1$ points along each dimension; however, we *oversample* by adding 1 point to each dimension for more representative models and more meaningful error estimates from these sampling points.
- To decide when to refine, the *type of error estimate* used to evaluate the polynomial fit is the maximum relative error across all sampling points. Alternatives, such as median or average, showed to insufficiently capturing highly localized inaccuracies.

2.3 Resulting Sub-space Partitionings

To illustrate the types of models generated by our approach, we once more consider `dtrsm`; more specifically: sub-models for `side = "L"`, `uplo = "L"`, `transA = "N"`, `alpha = 1`, and `m, n ∈ [8, 1024]`. Fig. 4 shows the partitioning of this 2D domain under different scenarios.

Figures 4a and 4b, respectively, show a rough and a fine sub-model for the Intel Penryn running OPENBAS. For the rough model, we relaxed the adaptive refinement by lowering the number of grid-points along each axis to 4 (i.e., oversampling of 0) and chose the average error as the termination criterion. The fine model corresponds to the aforementioned parameter choice. Comparing these two figures, we see how the refinement further subdivided the regions of insufficient accuracy, resulting in a better model.

Next, we apply the fine modeling configuration to different hardware and software: ATLAS [13] is modeled on the Penryn in Fig. 4c, while on an Intel Sandy Bridge-EP E5-2670,⁶ we used MKL [14] in Fig. 4d. Although each model is tiled in a quite different, unique way, all of them cover the performance characteristics of the corresponding BLAS implementation with estimation errors mostly well below 2%.

⁶ 3.3GHz (Turbo Boost), 8 cores, 20MB shared L3 cache, 8 flops/cycle.

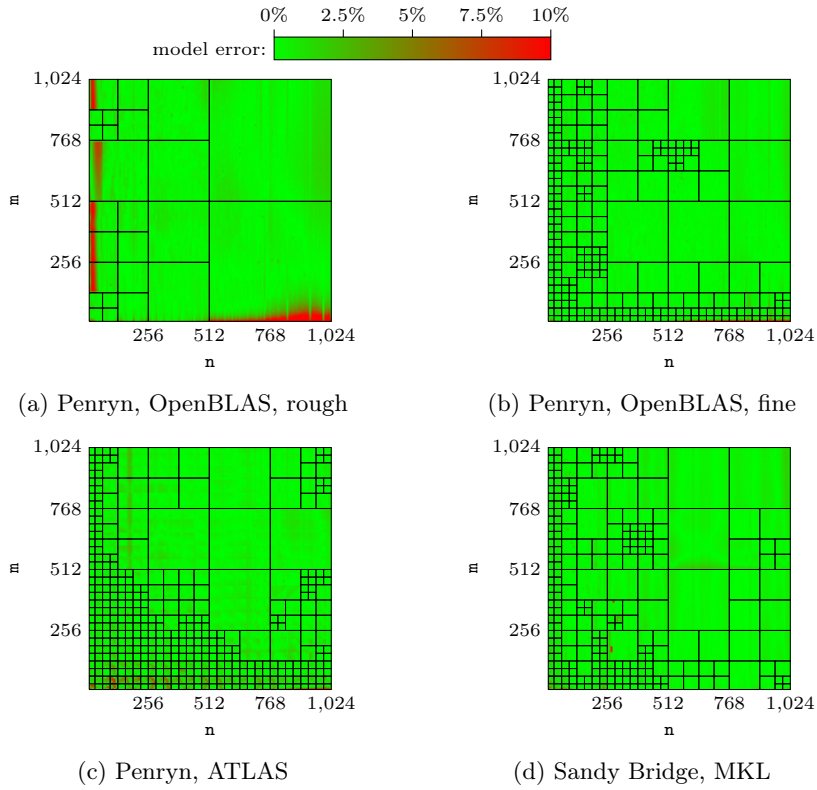


Fig. 4: Examples of sub-model domain partitioning for `dtrsmLLN`.

2.4 Trade-off: Accuracy vs. # Samples

In Fig. 5, we consider the three BLAS implementations OPENBLAS, ATLAS, and MKL and alter the adaptive refinement configuration parameters to highlight the variety of resulting performance models in terms of their accuracy and cost (i.e., number of samples) to generate them. The figure clearly shows the Pareto optimality in the trade-off between accuracy and cost. For each of these libraries, our framework can generate models of high accuracy with an average error⁷ below 0.5% and our selected configuration yields a good compromise between accuracy and model generation costs (#samples).

All performance measurements suffer from system fluctuations—small variations in performance resulting from uncontrollable interference from the execution environment, such as context switches. On our system, these fluctuations range from 1.2% for matrices of size 32×32 to 0.1% for size $1,024 \times 1,024$ —the same order of magnitude as the error in our models, which can be as low as

⁷ The error was computed by comparing the model estimates with measurements in each point of the covered domain that is a multiple of 8 along both m and n .

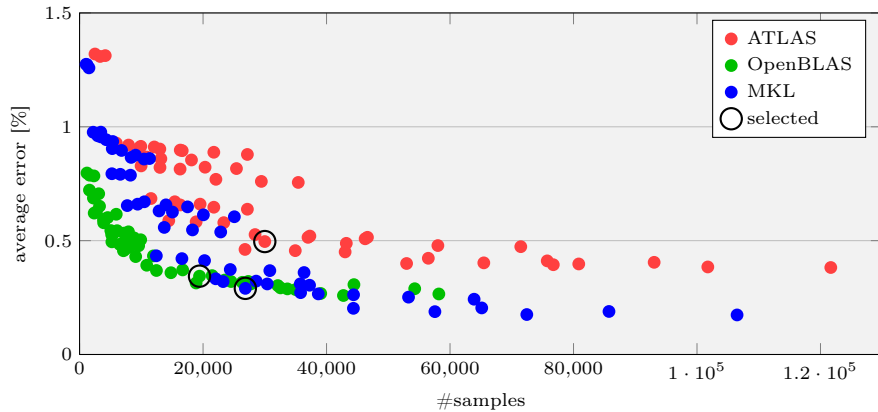


Fig. 5: Model accuracy vs. cost (`dtrsm` on Penryn).

0.2%. While we could strive for even higher accuracies by statistically accounting for system fluctuations at the cost of considerably more sample repetitions (cf. [5]), we refrain from doing so in this paper, since caching proves to have a significantly higher impact on performance.

2.5 Cache Unaware Prediction

Based on the generated performance models, we can attempt a first prediction of the performance of LAPACK’s QR decomposition `dgeqrf`. For this purpose, we consider the kernels composing this routine, estimate their runtime using performance models, and accumulate these runtime estimates into predictions. In Fig. 6, we present these resulting predictions for `dgeqrf` on a square matrix of size $n = 1,560$ (1 core of Intel Penryn, OPENBLAS) for both in-cache and out-of-cache models, alongside measurements of its runtime. As the figure shows, the in- and out-of-cache models, respectively, under- and over-estimate the measured runtime, a phenomenon observed across various scenarios involving different hardware, BLAS implementations and algorithms. In the following section, we introduce a cache tracking methodology that combines these two estimates and closes this gap.

3 Cache Modeling

The framework introduced in the previous section generates highly accurate performance models for dense linear algebra kernels. However, we have seen that this accuracy does not directly translate to accurate performance predictions for algorithms due to the influence of caching. In this section, we present a methodology to obtain high-quality performance predictions; specifically, we use a cache model that tracks which matrices or sub-matrices are in cache, and,

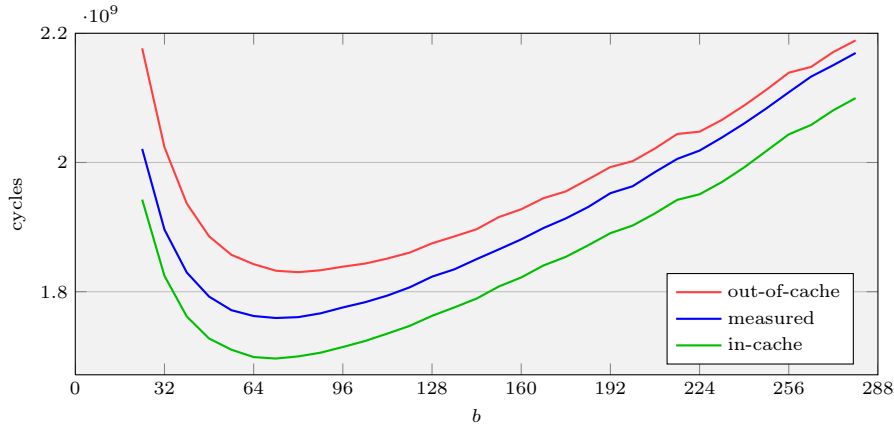


Fig. 6: Prediction of `dgeqrf`'s runtime from in- and out-of-cache models for square matrices of size $n = 1,560$ and varying block-size b .

based on this knowledge, obtain performance predictions through a weighted sum of the execution time estimates from in-cache and out-of-core models.

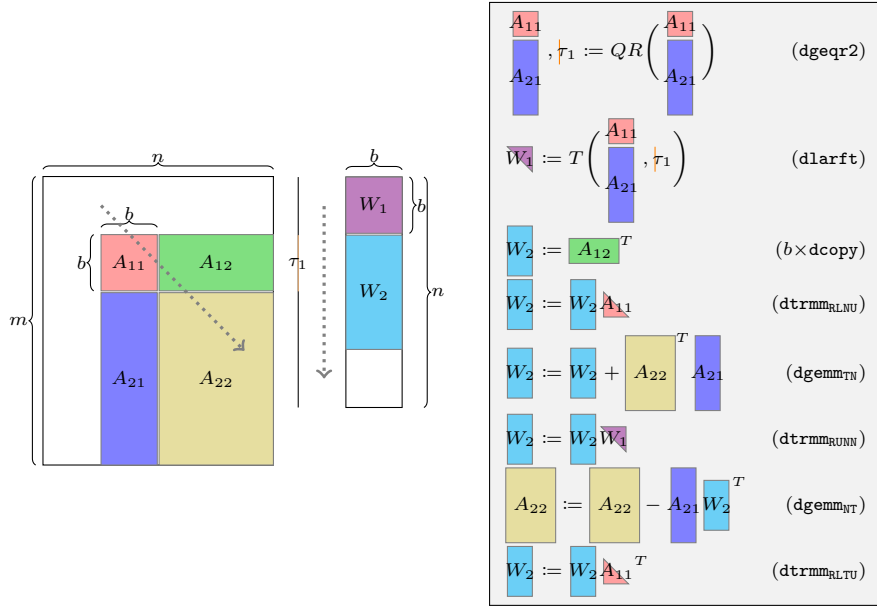
To illustrate the caching behavior we want to model, [Algs. 1](#) shows the exemplary blocked algorithm employed in LAPACK's QR decomposition `dgeqrf`. This routine decomposes the input matrix $A \in \mathbb{R}^{m \times n}$ as the product of an orthogonal matrix $Q \in \mathbb{R}^{m \times n}$ with an upper triangular matrix $R \in \mathbb{R}^{n \times n}$. Upon termination, R is stored in A 's upper triangular portion, while A 's lower portion, together with an additional output vector $\tau \in \mathbb{R}^{\min(m,n)}$, represent Q in the form of elementary reflectors. In terms of workspace, `dgeqrf` requires an auxiliary buffer $W \in \mathbb{R}^{m \times b}$, where b is the algorithmic block-size. `dgeqrf` traverses A in steps of this block-size b diagonally from the top left to the bottom right corner; at each step it operates on the sub-matrices A_{11} , A_{12} , A_{21} and A_{22} , on W_1 , W_2 , and τ .⁸

Our goal is to, for each kernel invocation (see [Algs. 1](#), right), determine if the involved sub-matrix operands are available in cache. For this purpose, we assume a fully associative Least Recently Used (LRU) cache replacement policy.⁹ With this policy, determining whether a memory region is in cache or not (or even in which cache level) boils down to accumulating the size of all memory regions loaded since and including its last access; if this size, referred to as the *access distance*, is smaller than the cache size, LRU guarantees that the considered memory regions is in cache.

Our first objective is to, within a sequence of compute kernels, identify the set of memory regions M that were accessed since the last operation involving a specified kernel operand \mathcal{O}_p . To this end, our approach scans backwards through

⁸ Note that the size of all these operands decreases from one iteration to the next.

⁹ Due to the regular storage format and memory access strides of dense linear algebra operations, this simplifying assumption does not affect the reliability of the results.



Alg. 1: QR Decomposition `dgeqrf`. The shapes on the left illustrate `dgeqrf`'s traversal of its data arguments A , τ , and W .

the previous kernel invocations, constructing the collection M of mutually exclusive memory regions from all encountered kernels. The scan terminates when either

- $\mathcal{O}p$ is found (all memory regions of the kernel containing $\mathcal{O}p$ are added to M),
- M is already larger than the cache size, or
- the beginning of the kernel sequence is reached (an artificial memory region as large as all operands of the entire predicted algorithm is added to M ¹⁰).

Independently of the termination condition, the resulting collection M contains all memory regions that were accessed since $\mathcal{O}p$ was last used. Computing and summing the sizes of these regions yields the access distance.

Example 2. In LAPACK's QR decomposition (Algs. 1), consider the `dtrmmRLNU` invocation

$$W_2 := W_2 A_{11}$$

For each of the two operands (W_2 and A_{11}), we now show how the access distance is computed by means of a backward scan of the kernels.

¹⁰ This reflects a repeated execution of the algorithm—the condition under which we perform our timings. Adapting this behavior to other scenarios would require knowledge on the surrounding program.

- W_2 was involved in the series of b `dcopys` immediately preceding the `dtrmmRLNU`. Hence, the scan terminates on condition 1. and since the last access to W_2 only the operands of these `dcopys` were loaded into cache:

$$M = \left\{ W_2, A_{12} \right\} .$$

- A_{11} is not involved in the `dcopys`, and the involved operands are (for reasonable block-sizes) not larger than the cache. Therefore the scan goes back to the previous kernel (`dlarft`), which happens to involve A_{11} . Once again, termination criterion 1. is met and the collection M for A_{11} is

$$M = \left\{ W_2, A_{12}, W_1, A_{11}, A_{21}, \tau_1 \right\} .$$

In contrast to this example, our method scans for the last access to a kernel operand not symbolically as sub-matrices but in the form of memory regions solely identified by their memory addresses and sizes. Hence, scanning works seamlessly across iterations of blocked algorithms, in each of which the symbolic sub-matrices refer to different memory regions.

Example 3. The first kernel invocation in each iteration of `dgeqrf` is `dgeqr2`:

$$\begin{matrix} A_{11} \\ A_{21} \end{matrix}, \tau_1 := QR \left(\begin{matrix} A_{11} \\ A_{21} \end{matrix} \right) .$$

- From one iteration of the blocked algorithm to the next, the shift in the blocking along the diagonal of A (see [Algs. 1](#), left) implies that (unless we are in the first iteration), the memory regions now associated with both A_{11} and A_{21} were in the previous iteration part of A_{22} . Therefore, an access is found in the second last kernel invocation `dgemmNT` and (with the symbolic shapes referring to the previous iteration) we have

$$M = \left\{ W_2, A_{11}, A_{22}, A_{21} \right\} .$$

- τ_1 on the other hand was never previously accessed, which is why the scan terminates on either criterion 2. (the collection of regions exceeds the cache size) or criterion 3. (the beginning of the algorithm is reached).

Once summing up the sizes of the corresponding collections M determines the access distances for all operands of a kernel, we weight the model estimates for the in-cache and out-of-cache execution times as follows: First, we translate

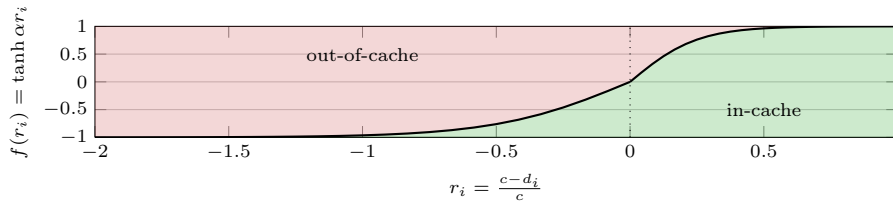


Fig. 7: Smoothing function f for in- and out-of-cache memory regions.

the access distance d_i of each memory region i into a *relative access distance* r_i with respect to the cache size¹¹ c :

$$r_i = \frac{c - d_i}{c} .$$

In other words, a relative access distance $r_i > 0$ means that region i is likely still in cache, while $r_i < 0$ means that it is likely no longer in cache. To avoid strict classification of in-cache or out-of-cache, we use a smoothing function f that splits operands with access distances close to the cache size between these extreme options (see Fig. 7):

$$f(r_i) = \tanh wr_i, \text{ where } w = \begin{cases} 4 & \text{if } r_i \geq 0, \\ 2 & \text{if } r_i < 0 \end{cases} .$$

Here, a value for f of 1 and -1 , respectively correspond to entirely in-cache and out-of-cache, while intermediate values indicate a distribution between both scenarios. Thus, $f(r_i)$ can be understood as a smoothed association with in- and out-of-cache preconditions for memory region i . From the $f(r_i)$ of each operand i , the cache-state association α for the entire kernel is obtained by weighting with the corresponding operand sizes s_i :

$$\alpha = \frac{\sum_i f(r_i) s_i}{\sum_i s_i} .$$

Now, the kernel runtime prediction p is obtained from in- and out-of-cache model estimates t_{ic} and t_{oc} as

$$t = \frac{1 + \alpha}{2} t_{ic} + \frac{1 - \alpha}{2} t_{oc} .$$

As the following section will show, this cache modeling approach yields accurate performance predictions for entire algorithms from only two cache-aware performance models for each kernel.

¹¹ We only consider the largest CPU cache, since the data movement between this cache and the main memory has the most critical influence on performance.

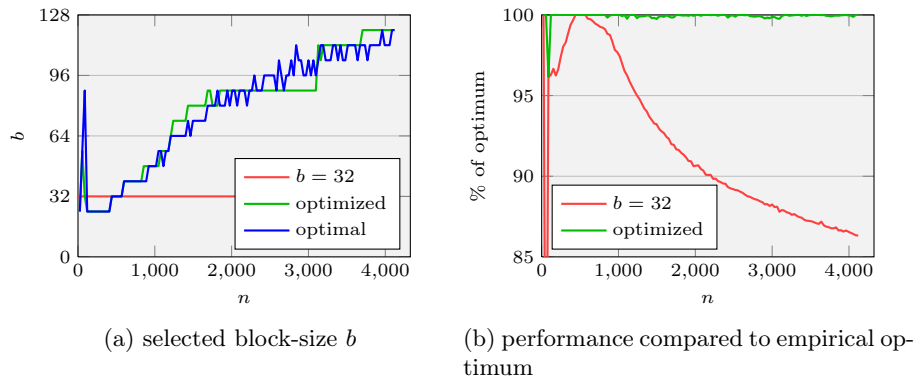


Fig. 8: Block-size optimization for `dgeqrf` (QR) on square matrices $A \in \mathbb{R}^{n \times n}$; Penryn, OPENBLAS, 1 thread.

4 Results

4.1 Block-size Optimization

In the introduction of this paper, we observed that LAPACK’s default block-size of can be severely suboptimal for algorithms such as the QR decomposition `dgeqrf` and the Cholesky decomposition `dpotrfL`. We now employ the methodology described in Sections 2 and 3 to predict optimal values for b . Given the size the input matrix, we estimate the runtime for the considered decomposition algorithm for a range of block-sizes b and accordingly pick the value that yields the best performance.

QR: Square Matrices. To evaluate the quality of our prediction, we consider `dgeqrf` on the Intel Penryn with OPENBLAS and square matrices $A \in \mathbb{R}^{n \times n}$ of up to size $n = 4,120$. In Fig. 8, we compare our prediction-based estimate for b with both LAPACK’s default ($b = 32$) and the empirically optimal¹² value. As Fig. 8a shows, the estimates for b closely match the optimum, even despite the visible fluctuations. Figure 8b presents how the performance with these optimized b compares to the empirical optimum: With the exception¹³ of $n = 88$, our prediction selects the block-sizes so well that we always attain at least 99.7% of the optimal performance.

QR: Tall-and-Skinny Matrices. Next, we consider `dgeqrf` for tall-and-skinny matrices $A \in \mathbb{R}^{4,120 \times n}$ —a common application of the QR decomposition—on the

¹² The performance measurements for this empirical optimization were very time-consuming and took more than 1 day.

¹³ The cause: up to this point, using only the unblocked version (i.e., $b = n$) is optimal, while our prediction already suggests the blocked algorithm with a small block-size.

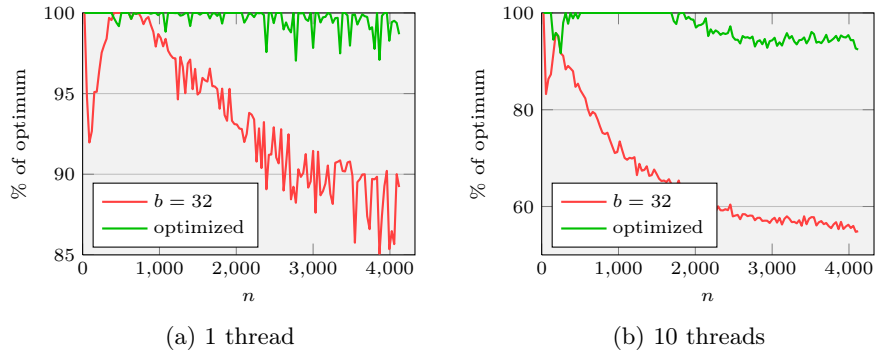


Fig. 9: Block-size optimization for `dgeqrf` (QR) on tall-and-skinny matrices $A \in \mathbb{R}^{4,120 \times n}$; Ivy Bridge-EP, OPENBLAS.

Intel Ivy Bridge-EP. Figure 9 displays how `dgeqrf` performs with our estimated block-size b compared to the empirically optimal block-size configuration, using single-threaded and multi-threaded BLAS. Due to the performance fluctuations from one problem-size to another on this system (reaching up to 5%), which are also clearly visible when using the default $b = 32$ (—), our predictions are less accurate compared to the older Penryn architecture; nevertheless, using 1 thread, our optimized block-size (—) still reaches around 99% of the optimal performance. Using all 10 cores, for large matrices, the efficiency only decays to 94%, and compared to LAPACK’s default block-size (—), the algorithm runs $1.6\times$ faster.

Cholesky. Fig. 10 contains the results for the block-size optimization for LAPACK’s Cholesky (`dpotrfL`) on 1 core of the Intel Penryn using OPENBLAS and MKL. For smaller matrices ($n \leq 3,500$), our optimization reaches 97% of the empirically optimal performance, and for large matrices, we reach well above 99%. The results are consistent across both BLAS implementations.

Together, these experiments provide evidence that our methodology indeed accomplishes our goal of optimizing the algorithmic block-size across a variety of different scenarios.

4.2 Cholesky Algorithm Selection

For a single mathematical operation, there usually exist several different algorithms [15, 16]. For such cases, performance predictions can distinguish the fastest algorithm without executing any of them. As an example, we consider the Cholesky decomposition ($LL^T = A$, $A \in \mathbb{R}^{n \times n}$ symmetric positive definite). We compare LAPACK’s `dpotrfL` with the four algorithms shown in Algs. 2: three blocked algorithms and a recursive one.

Like `dgeqrf`, the blocked algorithms traverse the matrix diagonally from the top left to the bottom right in steps of the prescribed block-size b ; for calls to

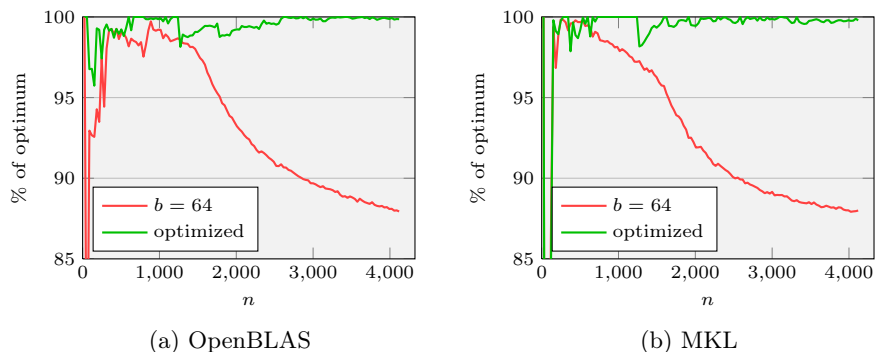


Fig. 10: Block-size optimization for `dpotrfL` (Cholesky) on $A \in \mathbb{R}^{n \times n}$; Penryn, 1 thread.

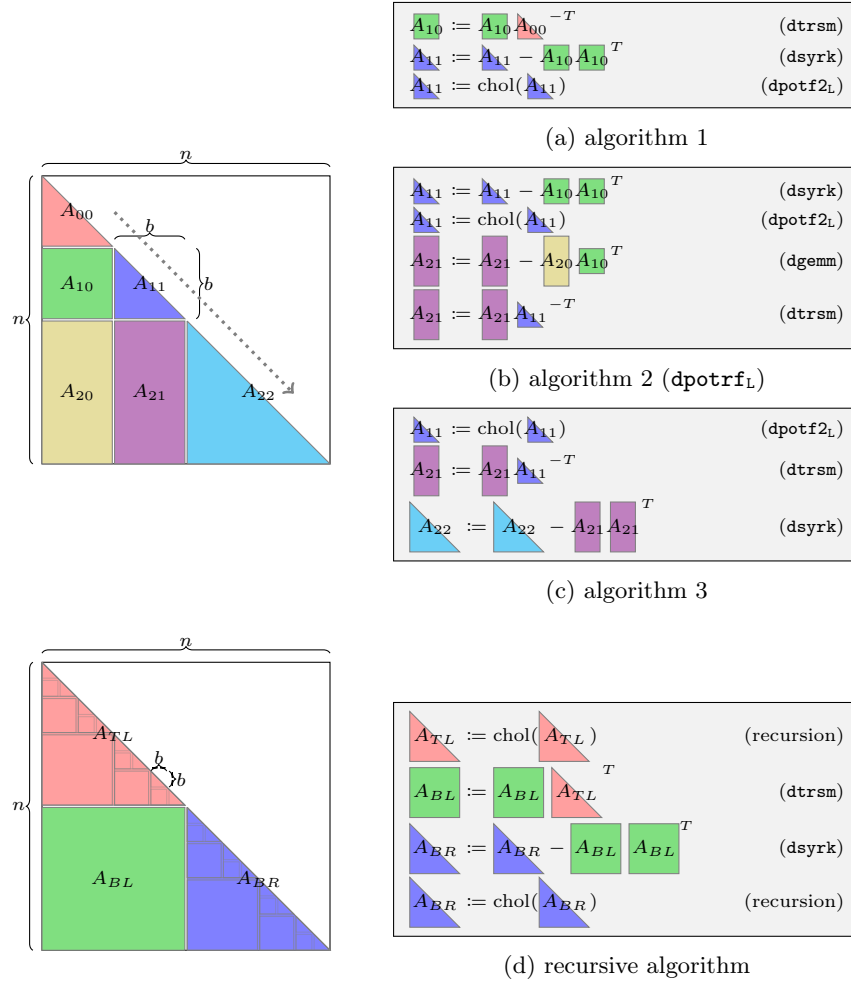
the unblocked algorithm on A_{11} , we use LAPACK’s `dpotf2L`. For these blocked algorithms, we use a moderate constant block-size of $b = 256$. The recursive algorithm cuts the matrix in the middle along both dimensions and recursively invokes itself for the decompositions of both A_{TL} and A_{BR} ; only once the size of these sub-matrices falls below the threshold block-size b , LAPACK’s unblocked `dpotf2L` is used. Preliminary experiments have shown that for this recursive algorithms, small block-sizes are the best choice irrespective of the matrix size;¹⁴ we therefore use $b = 24$.

Performance predictions and measurements of these Cholesky algorithms using single-threaded OPENBLAS on the Intel Penryn are presented in Fig. 11. LAPACK’s `dpotrfL` (—), which is identical to algorithm 2 (—), while not the slowest, turns out to be considerably slower than the fastest blocked algorithm 3 (—). Furthermore, the recursive algorithm (—) is the fastest by a considerable margin. Most importantly, however, our predictions rank the performance of all five algorithms is correctly.

Application of the Framework Combined into a single framework, our tools and methodology allow the following workflow: Given a dense linear algebra routine, such as those in LAPACK, the framework analyzes the involved compute kernels and, if needed¹⁵ generates or updates the collection of performance models. With the help of these models, the routine’s tuning parameters, such as the block-size, are then optimized, reaching within a few percent of the optimal performance. Moreover, when facing multiple, possibly automatically generated algorithms for one operation, our framework can both select the fastest algorithm and optimize it.

¹⁴ Small block-sizes do not penalize the performance as for blocked algorithms, where they entail a degradation in BLAS-3 performance on small and thin operands.

¹⁵ Different DLA operations and algorithms often offer a large overlap in terms of compute kernels.



Algs. 2: Algorithms for Cholesky decomposition.

5 Conclusion

In this paper, we presented a highly accurate performance prediction framework for dense linear algebra algorithms; this framework is based on two components: performance models for compute kernels and a cache tracking methodology. In doing so we extend our previous work [5] on performance model based predictions to algorithms whose operands exceed the cache size.

Our modeling framework generates measurement-based performance models for compute kernels, such as BLAS: Each routine's argument space is adaptively subdivided fitting performance samples with polynomial approximations until a sufficient degree of accuracy is reached. As a result, we obtain performance mod-

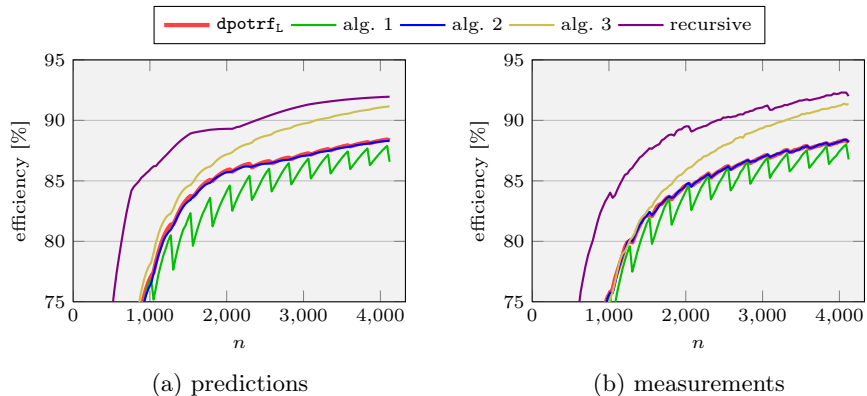


Fig. 11: Performance prediction and measurements for four alternative Cholesky implementations and `dpotrfL`.

els consisting of piecewise polynomials whose accuracy can match the magnitude of machine fluctuations.

In order to account for the cache locality of kernel operands, we combine performance models representing in-cache and out-of-cache situations. This combination is obtained by analyzing the sequence of kernel invocations in the target algorithm, deducing the cache locality of each of a kernel’s operands.

This methodology was shown to provide accurate performance predictions for several dense linear algebra algorithms. We used these predictions to optimize the algorithmic block-size for LAPACK algorithms and to select the fastest member within a family of mathematically equivalent algorithms.

Acknowledgments

Financial support from the Deutsche Forschungsgemeinschaft (DFG) through grant GSC 111 and the Deutsche Telekom Stiftung is gratefully acknowledged.

References

- [1] Anderson, E., Bai, Z., Bischof, C., Blackford, S., Demmel, J., Dongarra, J., Du Croz, J., Greenbaum, A., Hammarling, S., McKenney, A., Sorensen, D.: LAPACK Users’ Guide. Third edn. Society for Industrial and Applied Mathematics, Philadelphia, PA (1999)
- [2] Lawson, C.L., Hanson, R.J., Kincaid, D.R., Krogh, F.T.: Basic linear algebra subprograms for fortran usage. *ACM Trans. Math. Softw.* **5**(3) (September 1979) 308–323
- [3] Dongarra, J.J., Du Croz, J., Hammarling, S., Hanson, R.J.: An extended set of fortran basic linear algebra subprograms. *ACM Trans. Math. Softw.* **14**(1) (March 1988) 1–17

- [4] Dongarra, J.J., Du Croz, J., Hammarling, S., Duff, I.S.: A set of level 3 basic linear algebra subprograms. *ACM Trans. Math. Softw.* **16**(1) (March 1990) 1–17
- [5] Peise, E., Bientinesi, P.: Performance modeling for dense linear algebra. In: Proceedings of the 2012 SC Companion: High Performance Computing, Networking Storage and Analysis. SCC '12, Washington, DC, USA, IEEE Computer Society (2012) 406–416
- [6] Peise, E., Bientinesi, P.: A study on the influence of caching: Sequences of dense linear algebra kernels. In: Proceedings of the Ninth International Workshop on Automatic Performance Tuning. (July 2014)
- [7] OpenBLAS: <http://xianyi.github.com/OpenBLAS>
- [8] Cuenca, J., Giménez, D., González, J.: Architecture of an automatically tuned linear algebra library. *Parallel Comput.* **30**(2) (February 2004) 187–210
- [9] Iakymchuk, R., Bientinesi, P.: Modeling performance through memory-stalls. *SIGMETRICS Perform. Eval. Rev.* **40**(2) (October 2012) 86–91
- [10] Iakymchuk, R., Bientinesi, P.: Execution-less performance modeling. In: Proceedings of the Second International Workshop on Performance Modeling, Benchmarking and Simulation of High-Performance Computing Systems (PMBS11) held as part of the Supercomputing Conference (SC11), Seattle, USA (November 2011)
- [11] Whaley, R.: Empirically tuning lapack’s blocking factor for increased performance. In: Computer Science and Information Technology, 2008. IMCSIT 2008. International Multiconference on. (Oct 2008) 303–310
- [12] Lam, M.D., Rothberg, E.E., Wolf, M.E.: The cache performance and optimizations of blocked algorithms. In: Proceedings of the Fourth International Conference on Architectural Support for Programming Languages and Operating Systems. ASPLOS IV, New York, NY, USA, ACM (1991) 63–74
- [13] Whaley, R.C., Dongarra, J.J.: Automatically tuned linear algebra software. In: Proceedings of the 1998 ACM/IEEE Conference on Supercomputing. SC '98, Washington, DC, USA, IEEE Computer Society (1998) 1–27
- [14] Intel: <https://software.intel.com/en-us/intel-mkl>
- [15] Fabregat-Traver, D., Bientinesi, P.: Automatic generation of loop-invariants for matrix operations. In: Computational Science and its Applications, International Conference, Los Alamitos, CA, USA, IEEE Computer Society (2011) 82–92
- [16] Fabregat-Traver, D., Bientinesi, P.: Knowledge-based automatic generation of partitioned matrix expressions. In Gerdt, V., Koepf, W., Mayr, E., Vorozhtsov, E., eds.: *Computer Algebra in Scientific Computing*. Volume 6885 of *Lecture Notes in Computer Science.*, Heidelberg, Springer (2011) 144–157